HfN_2 monolayer: A new direct-gap semiconductor with high and anisotropic carrier mobility*

Yuan Sun(孙源)[1,†], Bin Xu(徐斌)[2,‡], and Lin Yi(易林)[3]

[1] School of Physics and Engineering, Zhengzhou University, Zhengzhou 450052, China
[2] School of Physics and Electronics, North China University of Water Resources and Electric Power, Zhengzhou 450011, China
[3] Department of Physics, Huazhong University of Science and Technology, Wuhan 430074, China

(Received 5 November 2019; revised manuscript received 8 December 2019; accepted manuscript online 12 December 2019)

Searching for two-dimensional (2D) stable materials with direct band gap and high carrier mobility has attracted great attention for their electronic device applications. Using the first principles calculations and particle swarm optimization (PSO) method, we predict a new 2D stable material (HfN_2 monolayer) with the global minimum of 2D space. The HfN_2 monolayer possesses direct band gap (∼1.46 eV) and it is predicted to have high carrier mobilities (∼10^3 $cm^2 \cdot V^{-1} \cdot s^{-1}$) from deformation potential theory. The direct band gap can be well maintained and flexibly modulated by applying an easily external strain under the strain conditions. In addition, the newly predicted HfN_2 monolayer possesses good thermal, dynamical, and mechanical stabilities, which are verified by *ab initio* molecular dynamics simulations, phonon dispersion and elastic constants. These results demonstrate that HfN_2 monolayer is a promising candidate in future microelectronic devices.

Keywords: HfN_2 monolayer, first principles, electronic structure, carrier mobility

PACS: 31.15.A–, 73.20.At, 68.55.ag **DOI:** 10.1088/1674-1056/ab610b

1. Introduction

Direct band gap and high carrier mobility of materials are the significant fundamental requirement for next-generation two-dimensional (2D) field effect transistors (FETs).[1–3] The 'star material' graphene has rapidly risen to be one of the hottest stars in materials science due to its excellent electronic properties and potential applications.[4] However, graphene is semimetallic, which lacks a band gap to switch current on and off in transistors. This has greatly hindered its applications in microelectronic devices.[5] MoS_2 monolayer owns a direct band gap for field effect transistors,[6] whereas it has low carrier mobility (10^2 $cm^2 \cdot V^{-1} \cdot s^{-1}$),[7] which is still much lower than that of silicon (1400 $cm^2 \cdot V^{-1} \cdot s^{-1}$). Although single-layer black phosphorus has a moderate direct band gap (1.51 eV)[8] and high carrier mobility (∼10^3 $cm^2 \cdot V^{-1} \cdot s^{-1}$),[5] its environmental instability (fast oxidation and light-induced degradation) leads to a major hurdle for black phosphorus based devices. Therefore, it is highly desired to find new 2D direct band-gap semiconductors with high carrier mobilities for development of microelectronics.

Transition metal nitride semiconductors have attracted considerable attention in recent years owing to their excellent physical properties and wide applications.[9–17] For instance, 2D MoN_2 shows ferromagnetism and undergoes a magnetic phase transition under applied strain.[18] YN_2 monolayer is the promising candidate for both spintronic and spin caloritronic applications.[19,20] TaN_2 monolayer possesses a robust FM ground state with high Curie temperature.[21] NbN monolayer was found to exhibit advantages for valleytronics.[22] TiN monolayer also possesses enhanced auxeticity and ferroelasticity.[23] Few-layered HfS_2 field effect transistors display excellent field effect responses.[24] Bulk HfN_2 possesses ductility and shows anisotropy up to high pressure.[25] HfN_x films were successfully prepared and are a promising candidate material for the "via last process" in through-silicon-via (TSV) technology.[26] Whether it is possible to prepare 2D HfN_2 remains an open problem.

In this work, using first-principles calculations and the particle swarm optimization method, we extensively investigate the possible structure of HfN_2 monolayer. On the basis of simulations, we demonstrate that the thermally, dynamically, and mechanically stable HfN_2 monolayer has several prominent merits: (i) a moderate direct band gap (1.46 eV); (ii) high carrier mobilities (∼10^3 $cm^2 \cdot V^{-1} \cdot s^{-1}$); (iii) a flexibly modulated band gaps under external strain (from 1.16 eV to 1.82 eV). This discovery renders HfN_2 monolayer a promising 2D material for applications in future microelectronics.

*Project supported by the National Natural Science Foundation (Grant No. U1404108), the Innovative Talents of Universities in Henan Province of China (Grant No. 17HASTIT013), the Basic and Frontier Technology Research Program of Henan Province of China (Grant No. 162300410056), and the Key Scientific Research Projects of Higher Institutions in Henan Province of China (Grant No. 19A140018).

†Corresponding author. E-mail: yuansun44@163.com
‡Corresponding author. E-mail: hnsqxb@163.com

2. Methods

A global search for the lowest energy stable structure for HfN_2 monolayer by using the particle-swarm optimization (PSO) method as implemented in CALYPSO code,[27] which has resoundingly predicted many two-dimensional (2D) structures.[3,28–33] More details have been added to the Supporting Information. The structure relaxations are performed using the density functional theory (DFT) with the Perdew–Burke–Ernzerhof (PBE)[34] exchange–correlation functional, as implemented in the Vienna *ab initio* simulation package (VASP).[35] A large plane wave cutoff energy of 500 eV with the energy precision of 10^{-5} eV and the force precision of 10^{-2} eV was used to ensure the convergence. A 30 Å vacuum slab to avoid spurious interactions in the z direction. To obtain accurate electronic properties, the hybrid Heyd–Scuseria–Ernzerhof functional (HSE06)[36] was also employed. Spin orbit coupling (SOC) was considered in the calculation of electronic band structure due to the existence of heavy elements. Phonon dispersion is obtained by the density-functional perturbation theory[37] and the first-principle MD simulations within the Canonical ensemble (NVT) ensemble with the time step of 1 fs at 300 K to evaluate the thermal stability. The temperature is controlled by using the Nosé–Hoover method.[38]

The carrier mobility μ was calculated based on the deformation theory.[39] The carrier mobility μ in 2D materials is given as $\mu_{2D} = \frac{2e\hbar^3 C_{2D}}{3k_B T|m^*|E^2}$, where $\hbar$ is the reduced Planck constant, C_{2D} is the elastic modulus, k_B is Boltzmann constant, T is temperature (set to be 300 K), m^* is the effective mass, and E represents the deformation potential constant along the transport direction. More detail information is shown in the supporting information.

3. Results and discussion

3.1. Structural properties

Figure 1(a) presents the top and side views of atomic structure for HfN_2 monolayer, in which each Hf atom is surrounded by six N atoms and the Hf atom is in the centers of N_6 trigonal prisms. The structure exposes $P\bar{6}m2$ symmetry (space group No. 187) with hexagonal lattice. The optimized lattice parameters are $a = b = 3.42$ Å and with Hf at 1f (2/3, 1/3, 1/2) and N at 2g (0, 0, 0.472), respectively. More detail parameters are shown in the Supporting Information (Table S1). Calculation of the electron localization functions (ELF) shows the electron distributions of this HfN_2 monolayer, as shown in Fig. 1(b). Clearly, the electrons are mainly distributed and well delocalized at center between N and Hf atoms, which suggests the strong covalency in Hf–N bonds.

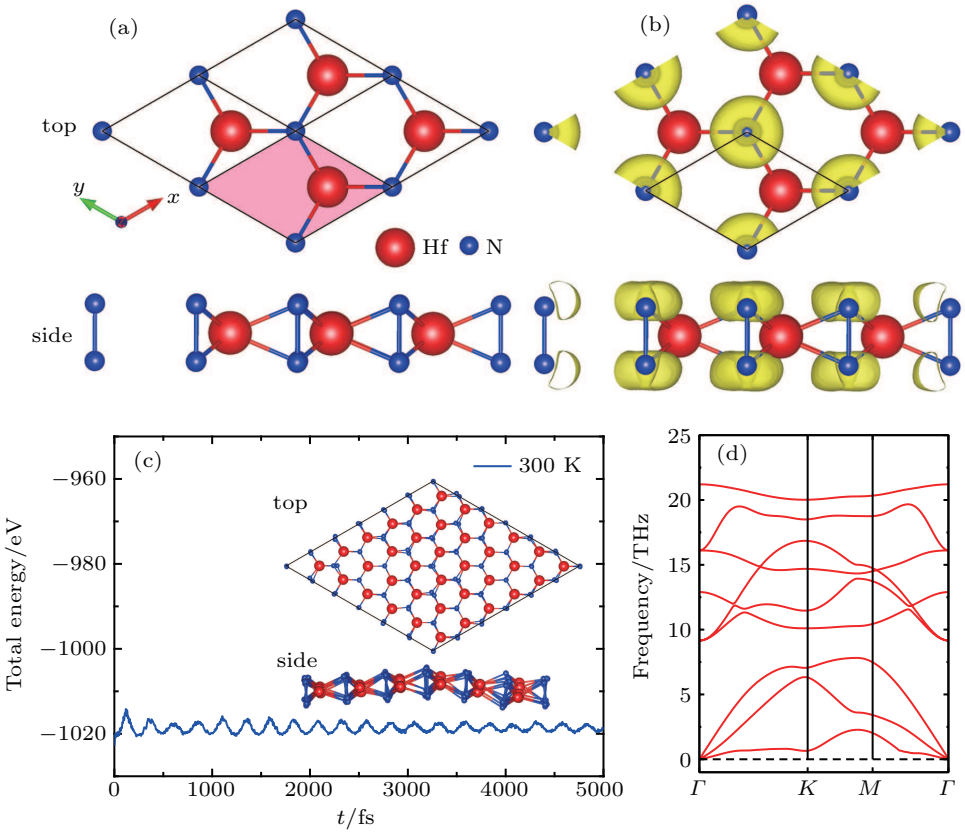

Fig. 1. (a) Top and side views of HfN_2 monolayer; (b) the electron localization function (ELF) with isovalue of 0.75; (c) fluctuation of total potential energy in the *ab initio* molecular dynamics (AIMD) simulation at 300 K, and (d) phonon dispersion of HfN_2 monolayer.

3.2. Stability properties

The stability of a crystal is important for the experimental fabrication. The thermal and dynamical stabilities of HfN_2 monolayer are first examined via *ab initio* molecular dynamics (AIMD) simulations and phonon dispersion. Figure 1(c) shows the fluctuations of the total potential energies and final structure of HfN_2 monolayer at 300 K for 5 ps. The small fluctuations of energy and integrity of original configuration confirm the thermal stability. Meanwhile, there is no imaginary mode in the whole Brillouin zone, suggesting the dynamic stability of HfN_2 monolayer (Fig. 1(d)). Noteworthy, the largest frequency of HfN_2 monolayer reaches up to 21.2 THz (708 cm^{-1}), which is greater than that in MoS_2 (473 cm^{-1}).[40] The large frequency strongly indicates the robust Hf–N interaction in HfN_2 monolayer. The good stabilities strongly suggest that 2D HfN_2 monolayer could survive at room temperature.

The mechanical properties is also examined by calculating the elastic constants. The elastic constants are $C_{11} = C_{22} =$ 149.4 N/m, $C_{12} = C_{21} = 90.3$ N/m, and $C_{66} = 29.4$ N/m. As a result, this monolayer also meets the mechanical stability Born criteria ($C_{11}C_{22} - C_{12}C_{21} > 0$ and $C_{66} > 0$) and has good in-plane stiffness. In-plane Young's moduli along x and y directions of HfN_2 monolayer, which can be deduced from the elastic constants by $E_x = (C_{11}C_{22} - C_{12}C_{21})/C_{22}$ and $E_y = (C_{11}C_{22} - C_{12}C_{21})/C_{11}$, are calculated to be 94.8 N/m, which is lower than that of graphene (334 N/m),[41] but higher than that of silicene (61 N/m).[42] High Young's modulus suggests the strong bonding nature. As E_x is equal to E_y, HfN_2 monolayer is mechanically isotropic. Poisson's ratio and Young's moduli as functions of the arbitrary direction in xy plane were presented in a 2D polar representation curve (Figs. 2(a) and 2(b)). This figure also shows the isotropic properties.

Although HfN_2 monolayer has good thermal, dynamic, and mechanical stabilities, this only means that it is a local minimum. Note that the global minimum structure has higher possibility to be realized in experimental process. Is the above discussed HfN_2 monolayer the global minimum on the 2D potential energy surface? To address this issue, the particle swarm optimization method was performed to global search for the lowest-energy stable structure for this monolayer. Our global search shows that the proposed HfN_2 monolayer has the lowest energy in our 2D global search space, which holds a great promise to obtain this monolayer experimentally.

3.3. Electronic properties

The band structure of the lowest-energy HfN_2 monolayer is shown in Fig. 2(c). Clearly, it is a semiconductor with a direct band gap. Both VBM and CBM locate at high symmetry K point. The PBE result gives a direct band gap of 1.46 eV, which is slightly smaller than that of MoS_2 (1.67 eV). Considering that the PBE functional usually underestimates the band gap, we recalculate the band structure of HfN_2 monolayer using the hybrid functional (HSE06) and find that the gap widens the gap to 2.68 eV (2.14 eV for MoS_2), as shown in Fig. S1. When considering the spin–orbit coupling (SOC) effect (Fig. S1), the band gaps reduce to 1.28 eV (PBE+SOC) and 2.45 eV (HSE+SOC). From Fig. S1, there is only a slight energy level splitting around the K point, and the overall SOC effect has a negligible influence on the band structure. Detailed analysis of different atomic components reveals that the conduction band minimum is dominated by orbitals of the Hf atom, whereas the valence band maximum is dominated by orbitals of the N atom. Due to the fact that the intrinsic physical properties would also be affected by the substrate and desirable band gap modulation, it is necessary to investigate the effect of external strain on the electronic properties of HfN_2 monolayer. Figure 3 shows the band gaps under biaxial strain (from -3% to 3%) for HfN_2 monolayer. Clearly, the external strain has a rather pronounced effect on the electronic structure, and the direct band gap can be well maintained. Under a biaxial compression strain, the band gap of HfN_2 monolayer increases with the increasing strain. While under tensile strain, the band gap decreases. Under the whole strains (from -3% to 3%), the band gaps decrease from 1.82 eV to 1.16 eV, which indicates that this monolayer can be flexibly modulated by applying an easily external strain. This property would endow it with a wider range of applications in optoelectronic devices.

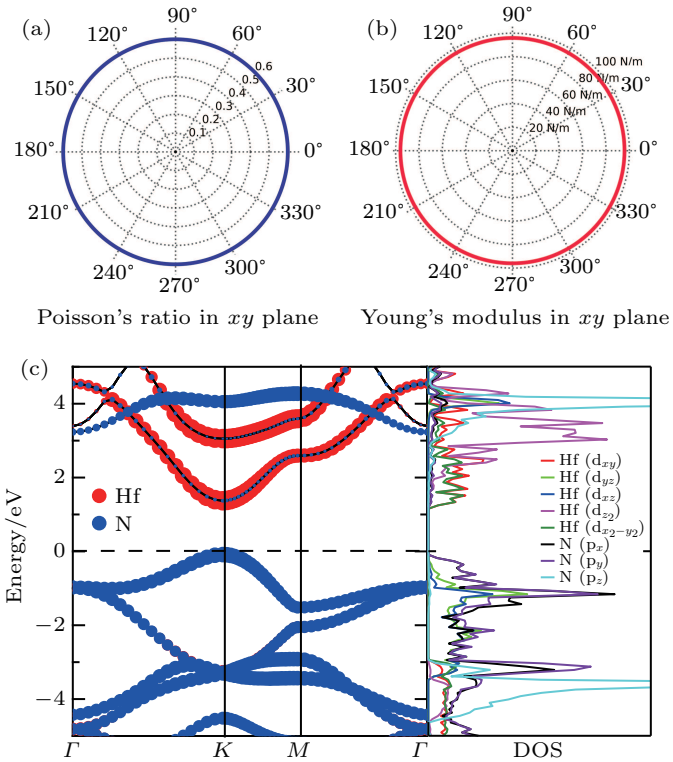

Fig. 2. (a) Calculated orientation-dependent Young's modulus and (b) Poisson's ratio; (c) projected band structure with corresponding density of states for HfN_2 monolayer at PBE level.

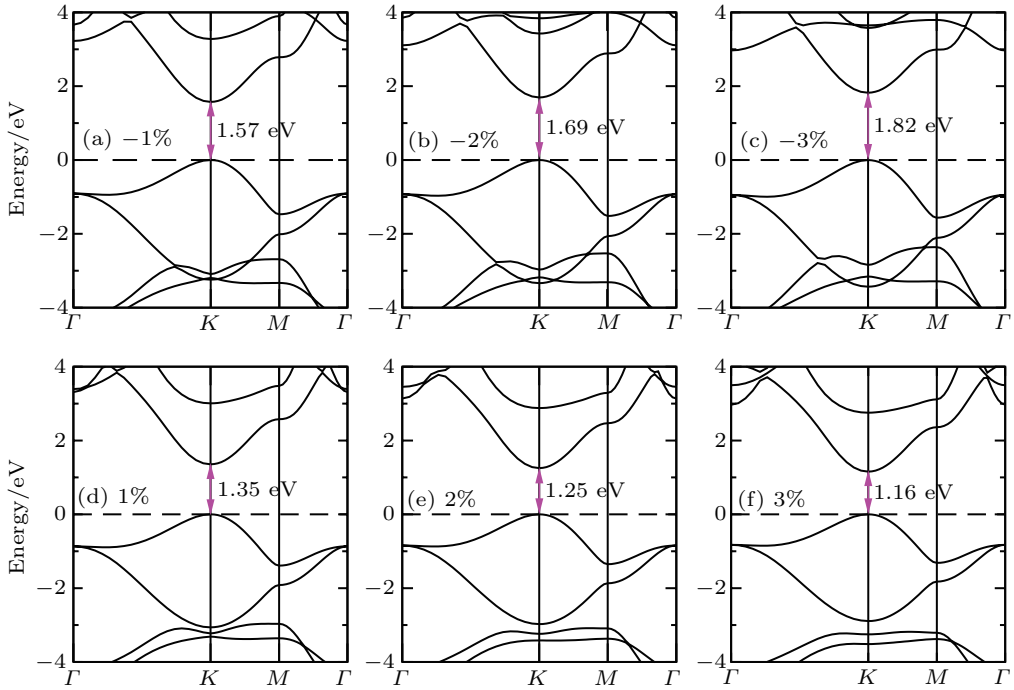

Fig. 3. Dependence of band gaps under biaxial strain (from −3% to 3%) for HfN_2 monolayer.

Table 1. Deformation potential constant E, elastic constant C_{2D}, effective mass m^*/m_e, and carrier mobility μ at 300 K for electrons and holes in HfN_2 monolayer.

		E/eV	C_{2D}/(N/m)	m^*/m_e	μ/cm^2·v^{-1}·s^{-1}
electron	x	–3.57	154.42	0.62	447
	y	–3.86	155.25	0.35	1206
hole	x	1.13	154.42	0.87	2262
	y	1.36	155.25	0.46	5464

As discussed above, HfN_2 monolayer possesses a highly stable and novel electronic structure. To further investigate its potential applications in 2D electronic and optoelectronic devices, its electron and hole mobilities at room temperature are calculated as presented in Table 1. The details for the electron mobility calculations are provided in the Figs. S2 and S3. According to Table 1, the in-plane stiffness of HfN_2 monolayer are 154.42 N/m and 155.25 N/m along the x and y directions, respectively, implying that this monolayer has isotropic mechanical properties. The achieved electron mobilities are 447 cm^2·V^{-1}·s^{-1} and 1206 cm^2·V^{-1}·s^{-1} along the x and y directions, respectively, which are much higher than that of MoS_2 (72.16 cm^2·V^{-1}·s^{-1} for x direction and 60.32 cm^2·V^{-1}·s^{-1} for y direction).[39] For holes, the mobilities are all higher than those of electrons, which are 2262 cm^2·V^{-1}·s^{-1} and 5464 cm^2·V^{-1}·s^{-1} along x and y directions, respectively. It is worth noting that the predicted hole mobilities are higher than electron mobilities, showing anisotropic behavior. From Table 1, it can be seen that the elastic modulus of x direction is almost equal to that of y direction. This anisotropic behavior is mainly originated from E and m^*. The small deformational potential constants are the main reason for the high carrier mobilities. The exceptionally high carrier mobility makes HfN_2 monolayer compelling candidates for applications in electronic devices.

4. Conclusions

In summary, using density functional theory computations and particle-swarm optimization techniques, we have successfully predicted a direct-band gap metal-nitride HfN_2 monolayer, which is highly stable and exhibits high intrinsic carrier mobilities. The direct band gap of 1.46 eV is close to that of MoS_2 (1.67 eV) at the PBE level, which is well maintained under external biaxial strains (from −3% to 3%). This direct band gap semiconductor is also confirmed by the hybrid functional with spin–orbit coupling effect (2.45 eV). In addition, this monolayer also possesses intrinsic acoustic-phonon-limited carrier mobility ($\sim 10^3$ cm^2·V^{-1}·s^{-1}), which is higher than that of MoS_2 monolayer. Interestingly, the mobility of holes is larger than that of electrons due to the small deformational potential constants. The direct band gap can be well maintained and flexibly modulated by applying an easily external strain. The robust direct gap and high carrier mobilities render 2D HfN_2 monolayer promising for future high-speed electronic and optoelectronic devices.

The supporting information gives the details about the lattice parameters of HfN_2 monolayer (Table S1), band structure of HfN_2 monolayer under different exchange–correlation functional (Fig. S1), and the details for the electron mobility calculations (Figs. S2 and S3).

References

[1] Xie M, Zhang S, Cai B, Zhu Z, Zou Y and Zeng H 2016 *Nanoscale* **8** 13407
[2] Wang B, Niu X, Ouyang Y, Zhou Q and Wang J 2018 *J. Phys. Chem. Lett.* **9** 487
[3] Zhang C and Sun Q 2016 *J. Phys. Chem. Lett.* **7** 2664
[4] Novoselov K S, Jiang D, Schedin F, Booth T J, Khotkevich V V, Morozov S V and Geim A K 2005 *Proc. Natl. Acad. Sci. USA* **102** 10451
[5] Li F, Liu X, Wang Y and Li Y 2016 *J. Mater. Chem. C* **4** 2155
[6] Mak K F, Lee C, Hone J, Shan J and Heinz T F 2010 *Phys. Rev. Lett.* **105** 136805
[7] Radisavljevic B, Radenovic A, Brivio J, Giacometti V and Kis A 2011 *Nat. Nanotech.* **6** 147
[8] Zhou Q, Chen Q, Tong Y and Wang J 2016 *Angew. Chem. Int. Ed. Engl.* **55** 11437
[9] Yu J, Wang L, Hao Z, Luo Y, Sun C, Wang J, Han Y, Xiong B and Li H 2019 *Adv. Mater.* **2019** 1903407
[10] Li F, Wang Y, Wu H, Liu Z, Aeberhard U and Li Y 2017 *J. Mater. Chem. C* **5** 11515
[11] Xiao X, Urbankowski P, Hantanasirisakul K, Yang Y, Sasaki S, Yang L, Chen C, Wang H, Miao L, Tolbert S H, Billinge S J L, Abruña H D, May S J and Gogotsi Y 2019 *Adv. Funct. Mater.* **29** 1809001
[12] Wang B, Wu Q, Zhang Y, Ma L and Wang J 2019 *ACS Appl. Mater. Inter.* **11** 33231
[13] Wei Y, Ma Y, Wei W, Li M, Huang B and Dai Y 2018 *J. Phys. Chem. C* **122** 8102
[14] Frey N C, Kumar H, Anasori B, Gogotsi Y and Shenoy V B 2018 *ACS Nano* **12** 6319
[15] Zhao W J and Xu B 2012 *Comput. Mater. Sci.* **65** 372
[16] Zhang C, Liu J, Shen H, Li X Z and Sun Q 2017 *Chem. Mater.* **29** 8588
[17] Gong S, Zhang C, Wang S and Wang Q 2017 *J. Phys. Chem. C* **121** 10258
[18] Wu F, Huang C, Wu H, Lee C, Deng K, Kan E and Jena P 2015 *Nano Lett.* **15** 8277
[19] Li J, Gao G, Min Y and Yao K 2016 *Phys. Chem. Chem. Phys.* **18** 28018
[20] Liu Z, Liu J and Zhao J 2017 *Nano Res.* **10** 1972
[21] Liu J, Liu Z, Song T and Cui X 2017 *J. Mater. Chem. C* **5** 727
[22] Anand S, Thekkepat K and Waghmare U V 2015 *Nano Lett.* **16** 126
[23] Zhou L, Zhuo Z, Kou L, Du A and Tretiak S 2017 *Nano Lett.* **17** 4466
[24] Chae S H, Jin Y, Kim T S, Chung D S, Na H, Nam H, Kim H, Perello D J, Jeong H Y, Ly T H and Lee Y H 2016 *ACS Nano* **10** 1309
[25] Zhang J, Jiang R, Tuo Y, Yao T and Zhang D 2019 *Acta Phys. Pol. A* **135** 546
[26] Takeyama M B, Sato M, Aoyagi E and Noya A 2014 *Jpn. J. Appl. Phys.* **53** 02BC05
[27] Wang Y, Lv J, Zhu L and Ma Y 2012 *Comput. Phys. Commun.* **183** 2063
[28] Zhang H, Li Y, Hou J, Du A and Chen Z 2016 *Nano Lett.* **16** 6124
[29] Wang B, Yuan S, Li Y, Shi L and Wang J 2017 *Nanoscale* **9** 5577
[30] Yin H, Liu C, Zheng G P, Wang Y and Ren F 2019 *Appl. Phys. Lett.* **114** 192903
[31] Wang B, Zhang Y, Ma L, Wu Q, Guo Y, Zhang X and Wang J 2019 *Nanoscale* **11** 4204
[32] Luo X, Yang J, Liu H, Wu X, Wang Y, Ma Y, Wei S H, Gong X and Xiang H 2011 *J. Am. Chem. Soc.* **133** 16285
[33] Gu T, Luo W and Xiang H 2017 *WIREs: Comput. Mol. Sci.* **7** e1295
[34] Perdew J P, Burke K and Ernzerhof M 1996 *Phys. Rev. Lett.* **77** 3865
[35] Kresse G and Furthmüller J 1996 *Phys. Rev. B* **54** 11169
[36] Heyd J, Scuseria G E and Ernzerhof M 2003 *J. Chem. Phys.* **118** 8207
[37] Baroni S, de Gironcoli S, Dal Corso A and Giannozzi P 2001 *Rev. Mod. Phys.* **73** 515
[38] Martyna G J, Klein M L and Tuckerman M 1992 *J. Chem. Phys.* **97** 2635
[39] Cai Y, Zhang G and Zhang Y W 2014 *J. Am. Chem. Soc.* **136** 6269
[40] MolinaS ánchez A and Wirtz L 2011 *Phys. Rev. B* **84** 155413
[41] Lee C, Wei X, Kysar J W and Hone J 2008 *Science* **321** 385
[42] Zhang H and Wang R 2011 *Physica B* **406** 4080